ELSEVIER

Thermochimica Acta 246 (1994) 1–10

thermochimica acta

Heat capacity anomalies at the Verwey transition of $Fe_{3(1-\delta)}O_4$

Shigeomi Takai [1], Tooru Atake, Yoshikata Koga*, [2]

Research Laboratory of Engineering Materials, Tokyo Institute of Technology, Nagatsuta-cho, Midori-ku, Yokohama 227, Japan

Abstract

It is known that the order of the Verwey transition changes from first to second, and then to a higher order, as the value of δ increases in magnetite, $Fe_{3(1-\delta)}O_4$. The associated heat capacity anomaly changes its shape and size, and it eventually becomes a broad hump, i.e. a higher order transition.

An attempt was made, with some success, at recovering the observed changes in heat capacity anomaly in terms of the two-state approximation, a generalized extension of the Strässler–Kittel treatment. By changing the adjustable parameters as a smooth linear function of δ, a qualitative trend of the observed changes in heat capacity anomaly was reproduced.

Keywords: Heat capacity; Magnetite; Transition; Verwey transition

1. Introduction

Although much research has been devoted to the Verwey transition of $Fe_{3(1-\delta)}O_4$ [1–8], understanding of the nature and mechanism of the transition is still limited. In particular, the charge distribution scheme of the low-temperature phase of

* Corresponding author: The Department of Chemistry, The University of British Colombia, Vancouver, B.C., V6T 1Z1, Canada.

[1] Present address: Department of Materials Science, Faculty of Engineering, Tottori University, Koyama, Tottori 680, Japan.

[2] On leave from: Department of Chemistry, The University of British Colombia, Vancouver, B.C. V6T 1Z1, Canada.

SSDI 0040-6031(94)01904-U

stoichiometric magnetite, $\delta = 0$, has not yet been determined. Yamada's model [3,6] could explain only some of the superlattice reflections [9], and the charge-ordering schemes proposed by Mizoguchi [4] and Iida [5] are apparently debatable [10].

An additional complication arises from non-stoichiometry in $Fe_{3(1-\delta)}O_4$. When the value of δ increases from 0 to 0.0039, the Verwey transition remains a first-order transition with a progressively smaller latent heat, and the transition temperature decreases gradually to about 109 K. For $0.0039 < \delta < 0.012$, the heat capacity anomaly becomes continuous and of a small hump type, indicating that the transition seems to change to second-order and then to higher order. The temperature at the top of the heat capacity peak decreases further to approx. 80 K [9].

The present paper concerns the effect of non-stoichiometry on the shape of the heat capacity anomaly. In the absence of an exact charge-ordering scheme in the low-temperature phase of stoichiometric magnetite, an attempt at understanding the effect of non-stoichiometry will be quite general and elementary. A detailed interpretation requires a fuller understanding of the Verwey transition of stoichiometric magnetite.

An attempt has been made by Honig and coworkers [11,12] to interpret the effect of non-stoichiometry on the order of transition, based on the two-state approximation formulated by Strässler and Kittel [13]. It should be pointed out that the condition imposed for the second-order transition to occur is too restrictive in the original work of Strässler and Kittel. As a result, the interpretation of Honig and coworkers [11,12,14,15] is not free from such restriction. One of us has previously generalized the Strässler–Kittel formulation [16,17]. Thus, the conditions for the second and higher order transitions were relaxed and a variety of heat capacity anomalies were recovered.

In this paper, we interpret the change in the nature of the Verwey transition induced by the change in the value of δ in terms of the generalized two-state approximation [16,17]. We emphasize that no new insight is expected for the nature of the transition. Rather, the change in the heat capacity anomalies is schematized in terms of a two-state approximation, in a more general form than in Ref. [12]. This provides a basis for future theoretical development.

2. Two-state approximation (general)

Here, we briefly summarize the treatment reported in Ref. [17]. The free energy per mole of a sub-system which is either in state A or state B is written as

$$F_m = (1-\rho)[f_A^\circ + RT\ln(1-\rho)] + \rho[f_B^\circ + RT\ln\rho] + F_m^E \quad (1)$$

where $\rho = N_B/(N_A + N_B)$ is the population density of state B, which serves as an order parameter, f_A° and f_B° are the molar free energies of state A and state B, respectively, and F_m^E is the excess molar free energy due to interaction among sub-systems. The mean field approximation is equivalent to

$$F_m^E = -0.5\rho^2\lambda \quad (2)$$

where λ is the mean field interaction parameter. Minimization of F_m with respect to ρ yields

$$F'_m = 0 = \varepsilon' - \lambda\rho - RT\left(\frac{s^\circ}{R} - \ln\frac{\rho}{1-\rho}\right) \tag{3}$$

where

$$f^\circ_B - f^\circ_A = \varepsilon^\circ - Ts^\circ \tag{4}$$

Eqs. (1)–(3) are identical to the formula given by Strässler and Kittel [13], with the identity

$$\frac{s^\circ}{R} = \ln(g_B/g_A) \tag{5}$$

where g_A and g_B are the degeneracy of states A and B respectively.

Rewriting Eq. (3)

$$\ln[\rho/(1-\rho)] = \left(\frac{\lambda}{RT}\right)(\rho - \varepsilon^\circ/\lambda) + s^\circ/R \tag{6}$$

Given ε°, λ and s°, the value of ρ can be obtained and the thermodynamics of the system fully described. In particular

$$E_m = \varepsilon^\circ\rho - \frac{\lambda}{2}\rho^2 \tag{7}$$

and

$$C_m = (\partial E_m/\partial T) = (\varepsilon^\circ - \lambda\rho)(\partial\rho/\partial T) \tag{8}$$

The solutions for ρ in Eq. (6) are the intersections of the following two curves in the ρ–z field, expressed as

$$z = \ln\frac{\rho}{1-\rho} \tag{9}$$

$$z = \frac{\lambda}{RT}(\rho - \varepsilon^\circ/\lambda) + s^\circ/R \tag{10}$$

See Fig. 1. Given λ, ε° and s°/R, Eq. (10) is a straight line with slope λ/RT going through a fixed point $W(\varepsilon^\circ/\lambda, s^\circ/R)$ on the ρ–z field. The conditions for first-order transition are equivalent to the case where the fixed point $W(\varepsilon^\circ/\lambda, s^\circ/R)$ is in the region above the line QS which is the tangent to the curve of Eq. (9), at point $Q(0.5,0)$. At the specific temperature T_c, the slope of the straight line, Eq. (10), becomes such that the line goes through point $Q(0.5,0)$. Therefore, at this temperature, there are three points of intersection, at $\rho = (0.5 - \Delta)$, 0.5, and $(0.5 + \Delta)$.

With $F''_m(0.5 - \Delta) > 0$, $F''_m(0.5) < 0$, and $F''_m(0.5 + \Delta) > 0$, the stable solutions are $\rho = 0.5 \pm \Delta$, and thus at this temperature the value of ρ jumps from $(0.5 - \Delta)$ to $(0.5 + \Delta)$, i.e. the first-order phase transition. Hence, the temperature of the

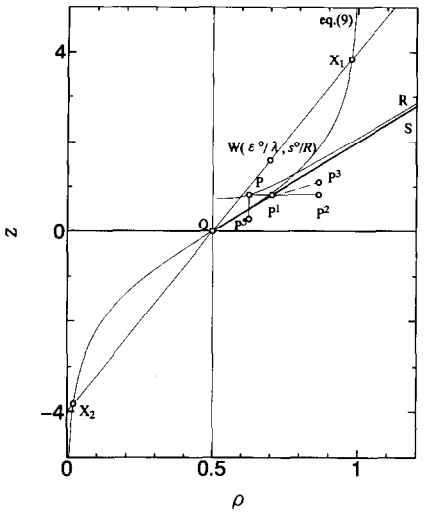

Fig. 1. Graphical solutions of ρ and the trace of point P with varying δ. Curve PR is the trace of point W satisfying the measured data, $T_V = 123.82$ K, $\Delta_{trs}H = 762.4$ J mol^{-1}, for $\delta = 0$. Line QS represents the locus at which the second-order phase transition occurs. P^1, P^2, P^3 and P^5 are the possible loci of point P.

Verwey transition T_V is this temperature T_c, i.e. $T_V = T_c$. The latent heat of transition can be calculated as

$$\Delta_{trs}E = E_m(0.5 + \Delta) - E_m(0.5 - \Delta) \tag{11}$$

If the fixed point $W(\varepsilon°/\lambda, s°/R)$ is on the line QS, the second-order transition occurs when the temperature becomes such that the straight line of Eq. (10) becomes identical to the line QS. With the single solution, $\rho = 0.5$, $F'''_m = F''''_m = 0$ and $F^{IV} > 0$ are satisfied. The undue restriction in the original work by Strässler and Kittel [13] was that $\varepsilon°/\lambda = 0.5$ and $s°/R = 0$, i.e. the fixed point W is identical to point Q in Fig. 1. This was their oversight and it was carried over to the works of Honing and coworkers [11,12,14,15]. Having relaxed the restriction and allowing the fixed point W to be anywhere on the line QS, a new situation arises.

When the fixed point W is located below the line QS (but above the abscissa), a higher order transition is manifested. Calculated heat capacity anomalies are shown below (in Fig. 4(a)) when the generalized two-state approximation is applied for $Fe_{3(1-\delta)}O_4$. It should be noted, however, that the temperature of the maximum of the heat capacity hump is lower than the temperature T_c at which the line of Eq. (10) goes through point Q in Fig. 1. From the experimental point of view, the locus of the maximum of the heat capacity hump is taken to be the transition temperature T_V. Thus, $T_V/T_c < 1$ for a higher order transition. Fig. 4(b) shows this situation. This is in contrast to the first- and second-order transitions, where $T_V/T_c = 1$.

3. Application to heat capacity anomalies of $Fe_{3(1-\delta)}O_4$

Heat capacity data for stoichiometric and non-stoichiometric magnetites were obtained by a relaxation method [9,18]. For stoichiometric magnetite, the most reliable C_p data were determined recently by adiabatic calorimetry [19], removing earlier confusions [20,21] regarding the shape of the C_p anomaly at the Verwey transition. The transition temperature was found to be 123.82 K and the latent heat of the transition 762.4 J mol^{-1}, with the additional contribution of the pre- and post-monitory C_p tails being 218.4 J mol^{-1} [18]. In comparison with the data in Ref. [9], the transition temperature is a few degrees higher, and the latent heat a few percent larger. From the fact that the value of T_V is the highest available, we believe that the sample used in Ref. [19] is the closest to the stoichiometry. We therefore use the data of Ref. [19] for stoichiometric magnetite, $\delta = 0$. For $\delta \neq 0$, data of Ref. [18] are used in this work as a general semi-qualitative trend. Because the reference made to the two-state approximation is rather crude and elementary, we only expect to determine a general trend in the changes in shape and location of the heat capacity anomaly as δ increases. We expect, however, that the parameters in the two-state approximation, i.e. $\varepsilon^\circ/\lambda$ and s°/R, change as a smooth function of δ. This contrasts with the treatment by Aragón and Honig [12] in which $s^\circ/R = \ln(g_B/g_A)$ was fixed at ln 2 for the first-order transitions, $\delta < 0.0039$, and then suddenly changed to ln 1 for $\delta \geq 0.0039$. The latter case is equivalent to having point W fixed at $Q(0.5,0)$ in Fig. 1. For such a case, the heat capacity anomaly at the second-order transition takes the triangular shape shown in Fig. 2. There will be no possibility of recovering a heat capacity anomaly of a smooth hump type. It should be noted that for the second-order transitions, heat capacity anomalies of various shapes can be recovered within the two-state approximation when point W is moved on the line QS, for example to (0.6,0.4) and (1.5,4) as also shown in Fig. 2.

3.1. $\delta = 0$

Because the pre- and post-monitory C_m tails due to the two-state approach with the mean-field approximation are considerably overestimated [16,17], we take into

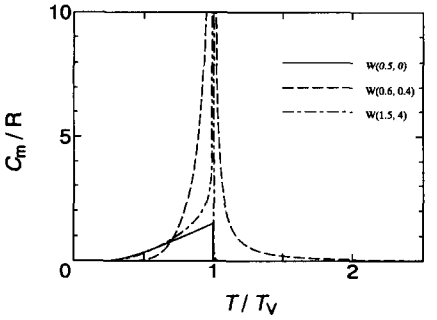

Fig. 2. Heat capacity anomalies due to generalized two-state approximations associated with the second-order transition.

account only the latent heat for the first-order transition. Due to Eq. (7), Eq. (11) is rewritten as

$$\Delta_{trs}E = 2\Delta(\varepsilon^\circ - \lambda/2) \tag{12}$$

At the transition point, T_V (or T_c), the slope is such that the line Eq. (10) goes through point $Q(0.5, 0)$. Therefore

$$\frac{s^\circ/R}{\varepsilon^\circ/\lambda - 0.5} = \frac{\lambda}{RT_V} \tag{13}$$

Also, the slope coincides with that of line X_1X_2 in Fig. 1. Namely

$$\frac{\lambda}{RT_V} = \frac{\ln\left(\frac{0.5+\Delta}{0.5-\Delta}\right) - \ln\left(\frac{0.5-\Delta}{0.5+\Delta}\right)}{(0.5+\Delta)-(0.5-\Delta)} = \frac{2\ln\left(\frac{0.5+\Delta}{0.5-\Delta}\right)}{2\Delta} \tag{14}$$

Given $\Delta_{trs}E = 762.4$ J mol^{-1} as Fe_3O_4 and $T_V = 123.82$ K for $\delta = 0$ [19], Eqs. (12), (13) and (14) yield the parameters $\varepsilon^\circ/\lambda$ and s°/R as a function of a possible value of Δ. In Fig. 1, the locus of $W(\varepsilon^\circ/\lambda, s^\circ/R)$ is shown as a function of Δ. At point P, the value of Δ is 0.45, and as Δ decreases, W moves towards R. Given a value of Δ, point W is fixed on the curve PR in Fig. 1 and hence the parameters $\varepsilon^\circ/\lambda$ and s°/R are fixed. As a result, all the thermodynamic properties can be calculated, including C_m, by Eq. (8). Fig. 3 shows the shapes of C_m with Δ as parameter. As is evident from Fig. 3, there is always a pre-monitory C_p tail present, but a post-monitory C_p tail decreases from $\Delta = 0.45$ and reaches zero at $\Delta \approx 0.3$ where point W lies on the curve of Eq. (9). Thereupon, it increases again as Δ decreases. It was found experimentally [19] that the post-monitory C_p tail was larger than the pre-monitory tail, reflecting the fact that a short-range order remains in the high-temperature phase [22]. The two-state approach with a mean-field approximation is incapable of dealing with a short-range order, since the order parameter ρ in the theory is of a global, or a long-range, nature. Moreover, a mean-field approximation inevitably overestimates pre- and post-monitory C_p tails. Therefore, we have no a priori method with which to determine the value of Δ by comparing pre- and post-monitory C_p tails with those observed. Nevertheless, it is clear Fig. 3 that when Δ decreases the size of pre- and post-monitory tails around the transition region becomes excessively large. Thus, we suggest tentatively that $\Delta = 0.45$ is a likely value, i.e. point W is placed at P in Fig. 1 for a stoichiometric sample.

3.2. $\delta \neq 0$

We propose that the parameters $\varepsilon^\circ/\lambda$ and s°/R change as a smooth function of δ in such a way that point $W(\varepsilon^\circ/\lambda, s^\circ/R)$ moves towards line QS in Fig. 1, whereupon the transition becomes second order. As point W moves away below the line QS, the transition become higher order. Line PP^1P^2 in Fig. 1 is one possibility, i.e. s°/R is kept constant. The range $0 < \delta < 0.0039$ corresponds to line PP^1, and $0.0039 < \delta < 0.012$ to P^1P^2. In the absence of a detailed theory, we assumed that W moves along the line PP^1P^2 linearly with δ. Hence $\overline{PP^1}/\overline{PP^2} = 0.0039/0.012$.

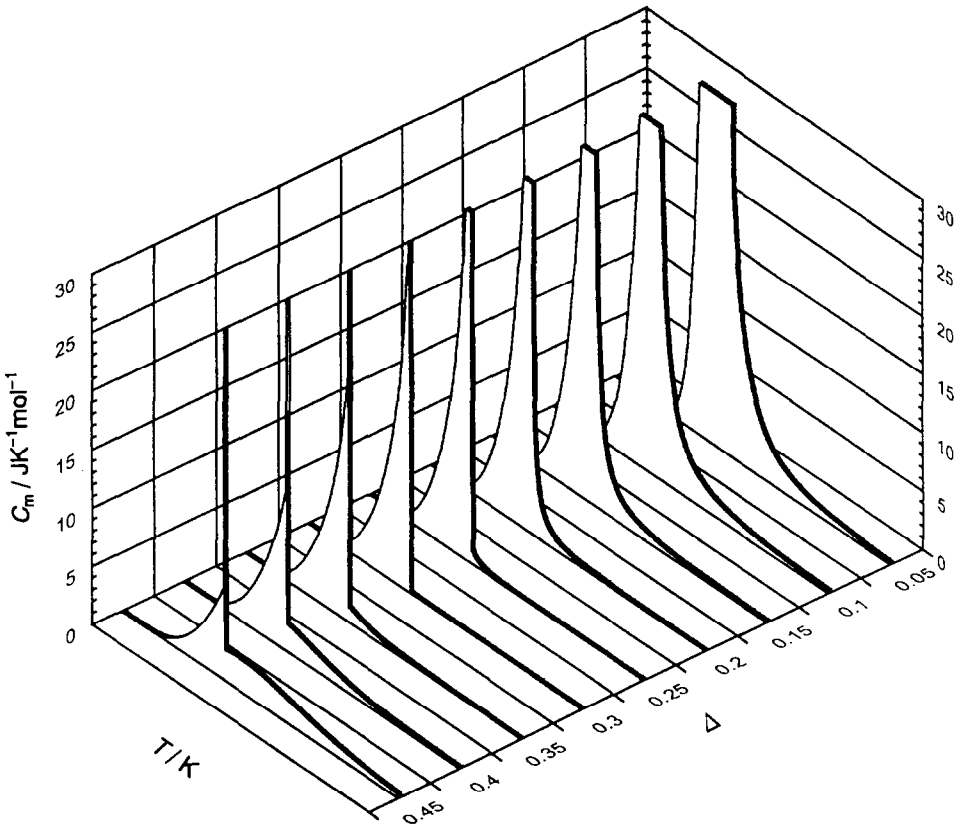

Fig. 3. Heat capacity anomalies for the first-order transition with several Δ. As Δ decreases from 0.45, point W moves from point P towards point R in Fig. 1.

Fig. 4(a) shows heat capacity anomalies as W moves from P to P^2. Fig. 5 shows the peak position of the heat capacity anomaly. In the higher order region, $\delta > 0.0039$, T_V decreases much faster than those observed. This may suggest that, rather than s°/R staying constant, it increases in such a manner as depicted by the broken line $P-P^1-P^3$. The heat capacity anomaly for P^3 is shown in Fig. 4(b) and the location of the peak in Fig. 5. Thus, the general trend of the heat capacity anomaly is qualitatively recovered if W moves from P to P^2 (or P^3) as δ increases from 0 to 0.012.

That the locus of W is $P-P^1-P^2$ (or P^3) is only a possibility. Point W could be made to move vertically in Fig. 1, i.e. $\varepsilon^\circ/\lambda$ is constant and s°/R decreases. However, as long as the assumption is kept that point W moves linearly with δ, it moves below the abscissa in Fig. 1 for a larger value of Δ, and hence there will be no transition. Therefore, this case was not considered. However, we point out that point W could move much more slowly below the line QS. When W reaches P^5 in

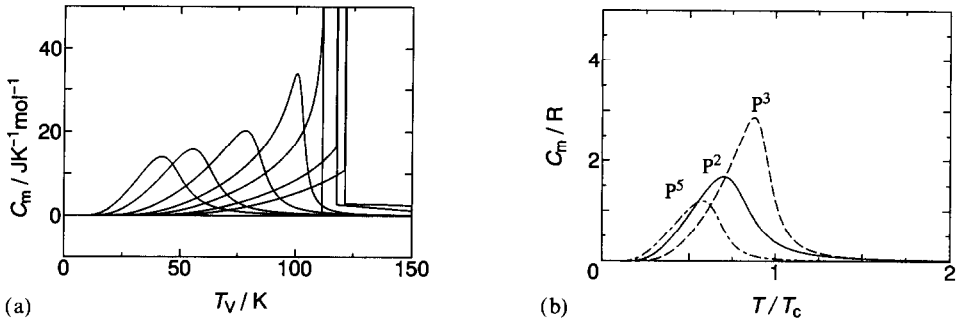

Fig. 4. Calculated heat capacity anomalies of magnetite. (a) For $\delta = 0.0068$, 0.0017, 0.0035, 0.0049, 0.0068, 0.0096 and 0.0121, respectively on the line $P-P^1-P^2$; and (b) for these values of δ at P^2, P^3 and P^5.

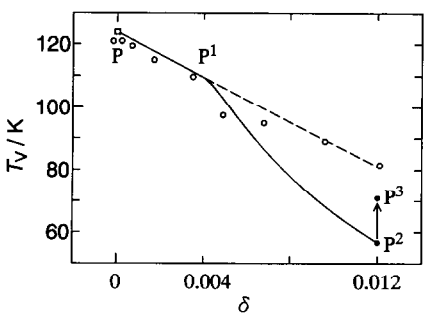

Fig. 5. T_V vs. δ plots: □, Ref. [19]; ○, Ref. [9]; solid line, this work.

Fig. 1, for example, which is on the line QP^2, the calculated heat capacity anomaly is shown in Fig. 4(b).

Table 1 summarizes all the numerical results due to the present treatment together with those observed [18,19]. The entropy of transition $\Delta_{trs}S$ was calculated by $\Delta_{trs}E/T_V$ for the first-order regime $\delta < 0.0039$, and as $\int_0^\infty (C_m/T)\,dT$ for $\delta \geq 0.0039$. The values of $\Delta_{trs}S$ are much higher than those observed for $\delta \geqslant 0.0039$, while those for $\delta < 0.0039$ are in reasonable agreement. This is due to the intrinsic weakness in the two-state approximation with mean field interactions, which overestimates the pre- and post-monitory contribution to the heat capacity anomaly. In particular, the heat capacity anomaly calculated by the two-state approximation contains the Schottky anomaly even if $\lambda = 0$, which amounts to a substantial contribution towards $\Delta_{trs}S$ ($R \ln 2$, if $s^\circ/R = 0$). In the present treatment, two states exist from $T = 0$ on, and hence the contribution to the population of the upper state exists from $T = 0$. This results in overestimation of the pre- and post-monitory tails of the heat capacity anomalies. However, in a real phase transition, the system behaves as if the two state is suddenly "created" in the vicinity of the phase transition [16,17].

Table 1
Observed and calculated Verwey transition temperature T_V and transition entropy $\Delta_{trs}S$. Observed data of stoichiometric and non-stoichiometric samples are taken from [18] and [17], respectively

δ	Observed		Calculated	
	T_V in K	$\Delta_{trs}S$ in J K^{-1} mol^{-1}	T_V in K	$\Delta_{trs}S$ in J K^{-1} mol^{-1}
1st order				
0	123.82	6.16	123.82	6.16
0.00021	121.0	5.80	123.1	6.06
0.00068	119.4	5.61	121.4	5.81
0.0017	115.0	5.21	117.8	5.08
0.0035	109.7	4.0	111.5	2.56
2nd order				
0.0039	–	–	110.1	9.59
Higher order				
0.0049	97.5	1.73	104.1	9.87
0.0068	95.0	1.63	90.1	9.86
0.0096	89.0	1.78	72.6	9.84
0.0121	81.5	0.77	60.2	9.83

Another important point to note is the relationship between the number of sub-systems and the formula unit of Fe_3O_4. The present treatment assumes they are equal, because we have no clear picture of state A or state B. But if the number of sub-systems is equal to $8 \times Fe_3O_4$ as a cubic unit cell or $32 \times Fe_3O_4$ as a unit cell of a low-temperature phase, the values of the Verwey transition entropy $\Delta_{trs}S$ for the higher order regime, $\delta > 0$, may become closer to those observed.

In summary, we point out that the original Strässler and Kittel paper imposes too strict a condition for the second-order phase transition [13], and as a result, the interpretation for the Verwey transition of $Fe_{3(1-\delta)}O_4$ by Aragón and Honig is unduly limited. When generalized [16,17], however, the two-state approximation could reproduce qualitatively the changes in the heat capacity anomalies, their sizes and shapes, by changing parameters smoothly with δ. Thus we provide a convenient starting point for a future theoretical development.

Acknowledgement

This research was supported by the Ministry of Education, Science and Culture, Japan in the form of a Grant-in-Aid for Scientific Research for T.A. and Guest Professorship for Y.K. at the Center for Ceramics Research, Research Laboratory of Engineering Materials, Tokyo Institute of Technology.

References

[1] E.J. Verwey, P.W. Haayman and F.C. Remijin, J. Chem. Phys., 15 (1947) 181.
[2] P.W. Anderson, Phys. Rev. B, 38 (1956) 1008.
[3] Y. Yamada, AIP Conf. Proc., 24 (1975) 79.
[4] M. Mizoguchi, J. Phys. Soc. Jpn., 44 (1978) 1501, 1512.
[5] S. Iida, Philos. Mag. B, 42 (1980) 349.
[6] Y. Yamada, Philos. Mag. B, 42 (1980) 377.
[7] E. Kita, Y. Tokuyama, A. Tasaki and K. Shiratori, J. Magn. Magn. Mater., 31–34 (1983) 787.
[8] K. Chiba and S. Chikazumi, J. Magn. Magn. Mater., 31–34 (1983) 813.
[9] J.P. Shepherd, J.W. Koenitzer, R. Aragón, J. Spalek and J.M. Honig, Phys. Rev. B, 43 (1991) 8461.
[10] M. Iizumi, T.F. Koetzle, G. Shirane, S. Chikazumi, M. Matsui and S. Todo, Acta Crystallogr. Sect. B, 38 (1982) 2121.
[11] J.M. Honig and J. Spalek, J. Solid State Chem., 96 (1992) 115.
[12] R. Aragón and M. Honig, Phys. Rev. B, 37 (1988) 209.
[13] S. Strässler and C. Kittel, Phys. Rev., 139 (1965) A758.
[14] J.M. Honig and J. Spalek, J. Less-Common. Met., 156 (1989) 423.
[15] J.M. Honig and J. Spalek, J. Solid State Chem., 96 (1992) 115.
[16] Y. Koga, Chem. Phys. Lett., 31 (1975) 571.
[17] Y. Koga, Coll. Phenom., 3 (1978) 1.
[18] R. Aragón, J.P. Shepherd, J.W. Koenitzer, D.J. Buttrey, R.J. Rasmussen and J.M. Honig, J. Appl. Phys., 57 (1985) 3221.
[19] S. Takai, Y. Akishige, H. Kawaji, T. Atake and E. Sawaguchi, J. Chem. Thermodyn., in press.
[20] E.F. Westrum, Jr. and F. Grønvold, J. Chem. Thermodyn., 1 (1969) 543.
[21] M. Matsui, S. Todo and S. Chikazumi, J. Phys. Soc. Jpn., 42 (1977) 1517.
[22] S.M. Shapiro, M. Iizumi and G. Shirane, Phys. Rev. B, 14 (1976) 200.